Semiconductor Optoelectronics
ISSN: 1001-5868

# THEORETICAL AND NUMERICAL STUDY OF THERMAL FLOW SENSOR TO RATIONALIZE ENERGY IN BUILDINGS

**Rouibah Abdelkader, Elbar Mohamed**
Faculty of Science and Technology, Applied Automation and Industrial Diagnostic Laboratory, University of Djelfa, Djelfa, Algeria.
a.rouibah@univ-djelfa.dz , rouibah_a@yahoo.fr , m.elbar@univ-djelfa.dz

**Chati Tounsi**
Faculty of Science and Technology, University of Djelfa, Djelfa, Algeria
tounsi1978chati@gmail.com

**ABSTRACT:**
In order to save energy, it is important to improve energy efficiency in construction while using it. To this end, the thermal flow sensor is used for real-time monitoring of heat transfer phenomena outside buildings.
In this work, a numerical simulation was carried out by ANSYS Fluent CFD software of a new and effective model of dynamic thermal flow sensors for quantitative characterization of the thermal exchange between the building's walls and the surrounding environment, the results obtained were compared to results in previous experimental and theoretical literature. There is a good compatibility of all results that allows dependence on numerical simulations in the future as a way of stewardship when studying energy rationalization.
**Keywords:** Thermal flow Sensor, performance thermal assessment, Thin-film sensor, Heat transfer.

## 1. INTRODUCTION:

Energy efficiency is about optimizing energy consumption, making it a rational use. Thus, improving energy performance has become necessary for buildings, equipment, etc. To do so, it is very useful to track in real time the phenomena of heat transfer outside buildings. The heat transfers between the walls and the surrounding environment depend on various climatic factors (wind, rain, infrared radiation, absorbed solar radiation...) which fluctuate constantly over time. Understanding heat flow and heat loss is inevitable when designing the buildings and engineering energy efficient floor heating systems. The heat flow is the rate of energy transfer through a given surface, and this amount can be measured by heat flux sensors, the latter is ideally suited for research in rationalizing and improving thermal efficiency.
Heat flow can be measured using multiple devices, including thermal flow sensors with electric dissipation or enthalpy, normal or tangential gradient [1-3]. It based primarily on the Fourier law.

To measure thermal flow and high surface temperature, a lot of sensor models based on thin thermal dual have been studied and developed [4-9]. B. Serio et al. [10] developed a model based on thin-film thermocouples made of gold palladium, to detect high temperatures of laser beam.

Fluxmeters based on thin-film thermos resistances have wide applications in monitoring and characterizing precision devices. Generally composed of very thin layers of a particular material such as: (Cu, Pt, Ni...), installed directly within the study area or according to electrically insulated, flexible or rigid, flat or cylindrical substrates. These Fluxmeters have been described extensively in many researches [11-15]. In which Hamadi and Amar [16] developed a new thermal metrology based on thin-film deposits for thermal characterization in microfluidics. Using a new calibration scheme based on blackbody, Clayton et al. [17, 18] developed model of high temperature thermopile-type heat flux sensor over a range of 448-1266 k.In the 1980s, Brunjail et al. [19] carried out experimental work at the Thermokinetics Laboratory on dynamic heat flux measurement sensors, where a new model, a pulse sensor, was developed to describe and monitor thermal exchanges between building walls and the surrounding environment at variable speed.

Bertrand [20] has designed a new dynamic heat flux sensor using a thin membrane heater and resistance thermometer instead of a wire heater and thermal double as suggested by Brunjail [19]. This new design provides a smaller time constant and a much easier manufacturing procedure and will facilitate the integration of new measurement procedures in the future. In the literature, there is not much work to deal with weather sensors using an integrated precision micro-heater.

Nguyen [21, 22] has designed a thermal sensor to measure the wind velocity and also its angular direction. Its thermal sensor is composed of thermocouples implemented in concentric rings on a disk with a heater on its center.

For the same purpose, Ruser [23] has used three resistance temperature sensor (RTS) based on semiconducting materials and the self-heating of the RTS crossed with different current intensity.

In fact, this developed model of sensors is an interesting type to improve the thermal management of buildings for the purpose of rationalizing energy consumption. Moreover, this designed sensor has the advantage of simplicity and little maintenance. This has prompted our great interest in studying this model numerically and theoretically and comparing the results with previous empirical results. From another perspective, in order to ensure proper analysis of heat transfers, experimental methods should not be relied upon alone but strengthened and monitored in computational and theoretical ways to ensure standard quality and neutrality.

## 2. Mathematical formulation

In this section we show equations that allow the development of heat transfer processes to be characterized globally under the effect of microclimate variability [24].The heat flux resulting from wall $\varphi_w$that characterizes all heat transfer phenomena (convection, radiation, evaporation…),presented by the following expression:

$$\varphi_w = \varphi_c + \varphi_r + \varphi_v + \alpha_s \varphi_s \qquad (1)$$

**2.1. Convective heat flux**

The convective heat flux is calculated by the following expression:

$\varphi_c = h_c(T_w - T_a)$ (2)

Where:

$h_c$isthe convective heat transfer coefficient.

**2.2. Infrared radiative heat flux**

The infrared radiative heat flux is calculated by the following expression:

$\varphi_r = h_r(T_w - T_r)$ (3)

Where:

$h_r$isthe radiation heat transfer coefficient as a function of the emissivities of the wall, the form factor and the mean temperature $T_m$.

**2.3. The heat flux produced by the evaporative process**

Thermal flux emitted by the evaporation process is provided by the following expression:

$\varphi_v = h_v(T_w - T_a) + \sigma_v$ (4)

Where:

$h_v$and$\sigma_v$are proportional to the latent heat of water vaporization, and dependent on the air temperature.

It may be noted that there is an analogy between convective heat transfers in dry air and mass transfers of water vapor under the concentration gradient; the concept of the boundary layer applies to both transfers: heat transfers in air, diffusion of water vapor in the air, and as the Schmidt number for this mass transfer is very close to the Prandtl number, the thicknesses of the thermal and mass boundary layers almost coincide.

**2.4. The heat flux of the sun's radiation**

Heat flux from sunlight $\varphi_s$is strengthened by the absorption coefficient $\alpha_s$of the walls. The total heat flow from the wall is supplied by the following expression after compensating the equations (2), (3), (4) in the equation (1):

$\varphi_w = h_c(T_w - T_a) + h_r(T_w - T_r) + h_v(T_w - T_a) + \sigma_v + \alpha_s\varphi_s$ (5)

In equation (5), full characterization requires different types of measurements, so the global heat transfer coefficient can be written as the following expression:

$h = h_c + h_r + h_v$ (6)

$\varphi_w = h(T_w - T_E)$(7)

Where:

$T_E$is the global ambient temperature.

Offset the equation (6) in equation (5) to read:

$$T_E = \frac{(h_c + h_v)T_a + h_r T_r - \alpha_s\varphi_s - \sigma_v}{h} \quad (8)$$

The sensor has a micro-heater that can supply a constant flux $\varphi_c$,Fig. (1a).The sensor temperature $T_c$is different from wall temperature$T_w$. The sensor temperature depends on

exchanges with the external environment but also on the temperature of the surrounding wall. The heat flow via the sensor is [19]:

$$\varphi_c = \varphi_w + h_0(T_c - T_w) = h(T_w - T_E) + h_0(T_c - T_w) + C\frac{dT_c}{dt} \quad (9)$$

Where:

*C* is the thermal capacity of the sensor.

If $\varphi_c = 0$and $C\frac{dT_{c0}}{dt} \approx 0$:

$$\varphi_w = h(T_w - T_E) \approx h_0(T_w - T_{c0}) \quad (10)$$

If $\varphi_c \neq 0$:

$$\varphi_c = h\theta + C\frac{d\theta}{dt} \quad (11)$$

Where: $\theta = T_c(t) - T_{c0}(t)$

For $= 0$ ; which solution with $\theta = 0$ is :

$$\theta = \frac{\varphi_0}{h_0}\left[1 - exp\left(-\frac{h_0}{C}t\right)\right] \quad (12)$$

The configuration shown in Figure(1b), at during its cooling phase we have the following expression for the surface temperature of the sensor [19]:

$$T_L - T_0 = \sum_{k=1}^{\infty} A_k \cos(u_k)\, e^{-\frac{au_k^2 t}{L^2}}\left[e^{-\frac{au_k^2 t_0}{L^2}} - 1\right] \quad (13)$$

The $u_k$ values are given using this following expression:

$$u_k \tan(u_k) = \frac{h_0 L}{\lambda} \quad (14)$$

Where:

*a* is the thermal diffusivity of an epoxy system.

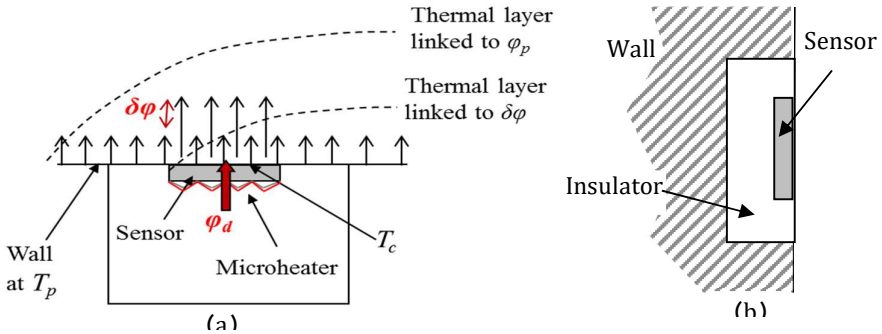


**Fig.1.**Thermal layer linked to the sensor heater (a) and position of the sensor in the wall (b)[19].

## 3. Geometrical description

In the experimental study carried out by Brunjail et al [19], the thermal flux sensor was installed in one of the walls of the wind tunnel. The sensor is exposed to air flow. Test section length 1.4m and has a cross-section 0.3×0.3 $m^2$. The sensor was operated in the wall with a distance of 0.6m from the inlet. To simulate the 2D geometry and to facilitate the study, the physical problem under consideration is summarized in Figure 2. We take the area closest to the sensor.

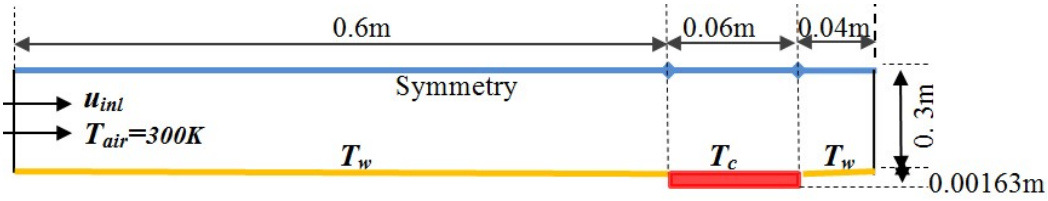


**Fig.2.**Geometry description of the sensor position (Study area).

## 4. Numerical model:

- Continuity equation:

$$\frac{\partial \rho}{\partial t} + div(\rho \vec{V}) = 0 \qquad (15)$$

- Momentum equation:

$$\rho \frac{\partial \vec{V}}{\partial t} = -\overrightarrow{grad}(P) + \mu \Delta \vec{V} \qquad (16)$$

Where:

$\mu$isdynamic viscosity of the fluid.

- Energy equation:

$$\rho C_P \frac{\partial T}{\partial t} + \vec{V}.\overrightarrow{\nabla T} = k\Delta \vec{T} + div(\bar{\bar{\tau}}.\vec{V}) \qquad (17)$$

Where:

$\bar{\bar{\tau}}$is the viscous stress tensor

## 4. Turbulence Modeling:

Menter (1993) [25] proposed a two-equation eddy-viscosity model of turbulence called SST k−ω, which based on the turbulent kinetic energy equations k, and the specific dissipation rate ω. This model can be employed as a Low-Reynolds number turbulence model to examine the flows and the heat transfer process. This model conjugates the k-ε turbulence model [26].The generic format for transport equations is [27]:

$$\rho\left[\frac{\partial k}{\partial t} + \frac{\partial}{\partial x_i}(k u_i)\right] = \frac{\partial}{\partial x_j}\left[\Gamma_k \frac{\partial k}{\partial x_j}\right] + \check{G}_k - Y_k \qquad (18)$$

$$\rho\left[\frac{\partial \omega}{\partial t} + \frac{\partial}{\partial x_i}(\omega u_i)\right] = \frac{\partial}{\partial x_j}\left[\Gamma_k \frac{\partial \omega}{\partial x_j}\right] + G_\omega - Y_\omega + D_\omega \qquad (19)$$

Where;

$\check{G}_k$and $G_\omega$; the production terms of$k$ and $\omega$.

$\Gamma_k$and$\Gamma_\omega$;the effective diffusivity of $k$ and $\omega$.
$Y_k$and $Y_\omega$; the dissipation terms of $k$ and $\omega$.
$D_\omega$ ; the cross-diffusion term.

## 5. Simulation results:

In this part, the ANSYS Fluent CFD software is applied to quantitively simulate of the thermal flux sensor with six different air velocities (2m/s ≤$u_{inlet}$≤12m/s) in the wind tunnel inlet. To improve the standard features of the CFD code, we have a User-Defined Function about heat flux profile applied to the surface of the thermal flux sensor. In the C language program, the function (UDF) was written and integrated into the solver of ANSYS Fluent. The function of the heat flux due to the micro-heater is defined in the equation(11), the solution of (11) is:

$$\theta = \frac{\varphi_0}{h_0}\left(1 - exp\left[-\frac{h_0}{C}t\right]\right) \qquad (20)$$

The sensor does not have time to cool completely between two successive pulses, a established periodic regime in which the temperature sensor oscillates between twovalues$\theta_M$and$\theta_m$.The record of$\theta = (T_c - T_{c0})$allows to calculate $h_0$ and$T_{c0}$.[28]
All governing equations of heat transfer were solved in turbulent regime using a CFD code. The general fluent settings, spatial discretization methods and Under-Relaxation factors were selected to solve the momentum and energy equations, as shown in tables (01, 02 and 03).The computations were simulated to be converged at $10^{-6}$ of root mean square residual values.

**Table 1.**General Fluent Settings

| | |
|---|---|
| Time Dependency | Transient |
| Solver Type | Pressure-Based |
| Model | Viscous-SST K-Omega |
| Pressure-Velocity Coupling | SIMPLE |
| Time Stepping Method | Fixed |

**Table 2.** Spatial Discretization Methods

| | |
|---|---|
| Gradient | Least square Cell Based |
| Pressure | Standard |
| Momentum | Second Order Upwind |
| Turbulent Kenitic Energy | Second Order Upwind |
| Specific Dissipation Rate | Second Order Upwind |
| Energy | Second Order Upwind |

**Table 3.**Under-Relaxation Factors

| | |
|---|---|
| Pressure | 0.3 |
| Density | 1 |
| Body force | 1 |
| Momentum | 0.7 |
| Turbulent Kenitic Energy | 0.8 |
| Specific Dissipation Rate | 0.8 |
| Turbulent Viscosity | 1 |
| Energy | 1 |

## 6. Meshing sensitivity analysis

The choice of mesh plays a very important role in the accuracy of the results and in the calculation time. It is therefore a question of making a study of the sensitivity of the results to the mesh in order to choose the one that gives good results without being very expensive in terms of calculation and storage memory. It is important that the mesh near the wall is properly sized to ensure accurate flow simulation.

Therefore, the first cell height calculations of the net outside the wall needed to obtain the required $Y^+$ using the flat plate boundary layer theory, as shown in table (04).

**Table 4.**Grid spacing for $Y^+$ as a function of velocity.

| Velocity (m/s) | Wall spacing |
|---|---|
| 2 | 1.45E-04 |
| 4 | 7.64E-05 |
| 6 | 5.24E-05 |
| 8 | 4.01E-05 |
| 10 | 3.26E-05 |
| 12 | 2.75E-05 |

In the initial step of the CFD simulations, to choose the best mesh, we have made some numerical simulation in which the variation of heat transfers coefficient $h_0$ as a function of number of nodes (49752, 67872, 85992, 104112, and 122232). The thermophysical properties of the sensor are: $\rho$=2249.15 kg/m$^3$, $C_p$=717.38 J/kg.K, $\lambda$=0.46 w/m.K.

Figure (3) shows the grid independence at air velocity (v=2m/s) and effect on heat transfer coefficient. We observe the stability of the results of heat transfer coefficient $h_0$ between mesh 5 and mesh 4. Therefore, we select mesh 4 with (104112) nodes to perform the numerical simulation of our study. Figure (4)

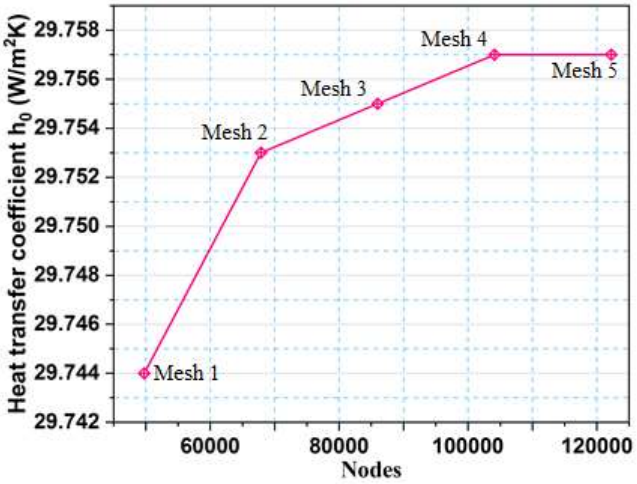


**Fig.3.**Grid independence at air velocity (v=2m/s) and effect on heat transfer coefficient $h_0$.

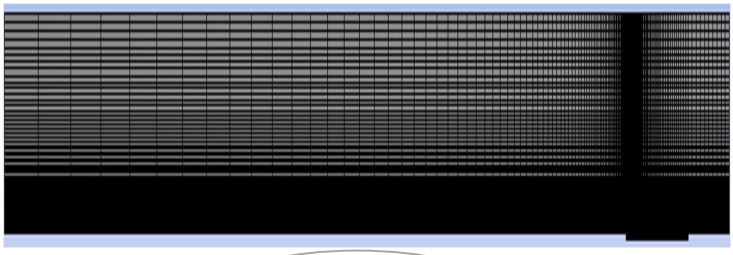

**Fig.4.** Grid meshing

In order to choose the time step, the simulation was performed in the same boundary terms with only changing the time step of the calculation ($\Delta t = 0.1s$ and $0.01s$), (Table5).
Figure (5) shows the evolution of heat transfer coefficient $h_0$ values by air velocity for each step of time,there is no obvious difference in results depending on the size of the Δt time step, and also when assessing the error rate between experimental results and CFD numerical results, Figure (6), so the size of the time step (Δt=0.1s) was selected to implement all simulations.

**Table 5**.Velocity effect on heat transfer coefficient $h_0$

| Velocity(m/s) | 2 | 4 | 6 | 8 | 10 | 12 |
|---|---|---|---|---|---|---|
| $h_0$ $(\Delta t = 0.1s)$ | 29.032 | 44.236 | 56.545 | 67.932 | 77.69 | 86.5 |
| $h_0$ $(\Delta t = 0.01s)$ | 29.955 | 44.4996 | 56.545 | 67.932 | 77.5587 | 86.362 |

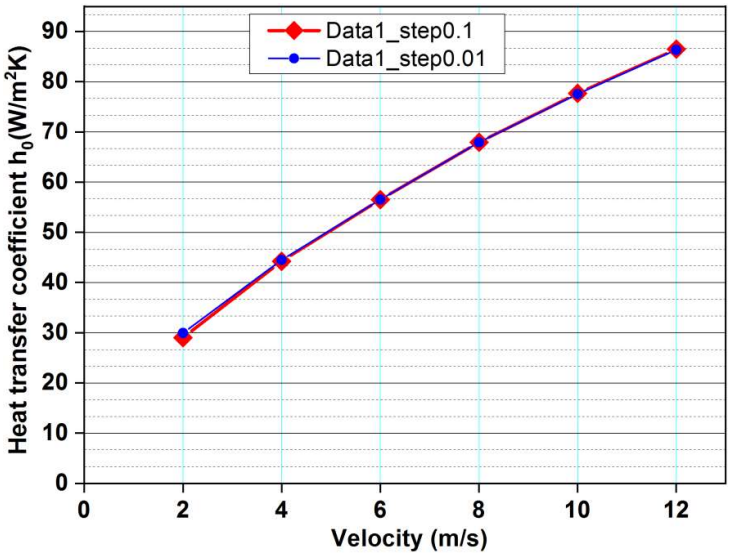


**Fig.5**. Velocity effect on heat transfer coefficient $h_0$

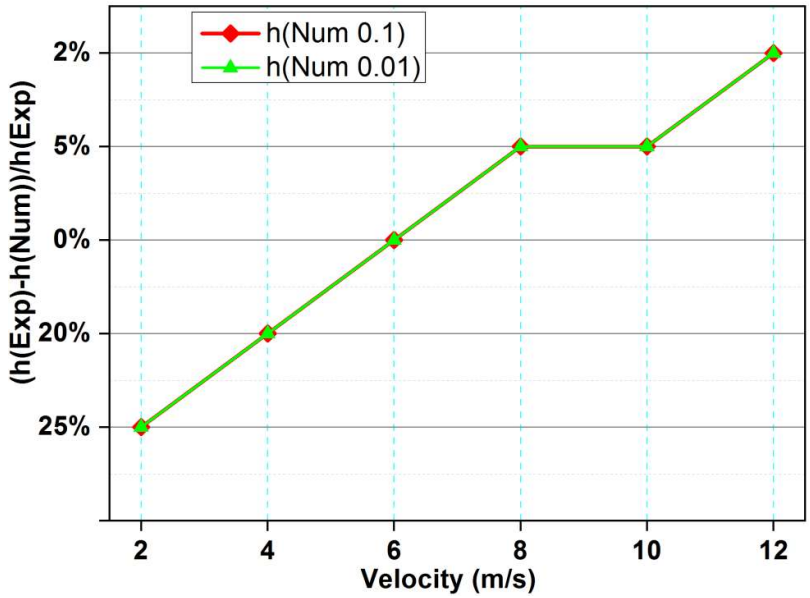


**Fig.6.**Represents error rate between Experimental results [19] and CFD numerical results.

Figure (7) represents a comparison of the values of the heat transfer coefficient obtained from the numerical simulation of CFD in our study with the results of previous studies [19,20], there are some differences between numerical simulation results in our study and Brunjail experimental results [19], but there is good compatibility with Bertrand experimental results [20]. There is also a slight difference recorded for Brunjail theoretical results [19] where greater values of heat transfer coefficient appear in our results.

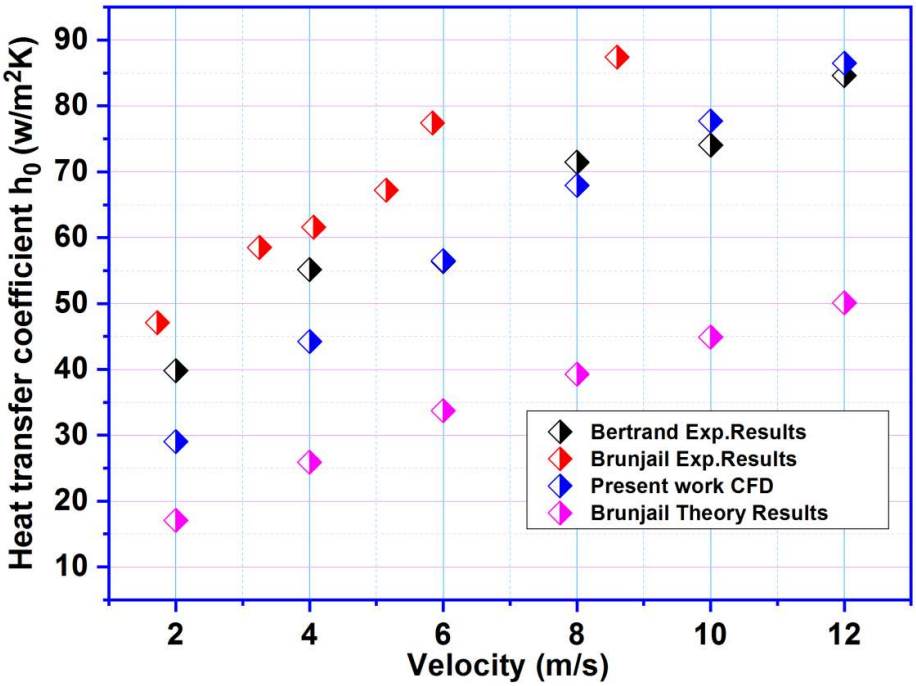


**Fig. 7.** Comparison of numerical simulation values of heat transfer coefficient $h_0$ with experimental results and theoretical values.

## 7. Calculation of the theoretical heat transfer coefficient $h_0$

The expression established by Leveque seems to us usable for determining the local coefficient of convection linked to a disturbance $\delta T_w$.The tangential stress due to the friction of the air on the plate is written:

$$\tau_w = \mu \frac{\partial u}{\partial y} = \mu\gamma \quad (21)$$

$$\tau_w = \left(\frac{0.893}{\lambda}\right)^3 9a(x - x_0)h^3_{0c(x-x_0)} \quad (22)$$

Where; $\mu$ is a dynamic air viscosity.

The coefficient of friction in turbulent conditions $C_f$ is (Blasius formula)

$$C_f = \frac{2\tau_p}{\rho u_\infty^2} = \frac{0.059\,2}{Re_x^{0.2}} \quad (23)$$

Where: $\rho$ ; is the density of air.

We deduce the Nusselt linked to the boundary layer

$$Nu_{0(x-x_0)} = \frac{h_{0c(x-x_0)}(x - x_0)}{\lambda} \quad (24)$$

From which;

$Nu_L = 0.0213Pr^{1/3}Re^{0.6075}$ (25)

Table (6) shows that comparing the values of results obtained theoretically with the correlation, the values of coefficients (*A*=0.0213) and (*m=0.6075)* obtained in this theoretical approach give a good compatibility that can be relied upon.

Figure (8) illustrates the theoretical relationship between *ln(Nu)* and *ln(Re),* which well illustrates this good relationship link.

**Table 6.** Comparison of our results with a correlation

| V (m/s) | h (W/m²K) | Nu | Re | Ln (Nu) | Ln (Re) |
|---|---|---|---|---|---|
| 2 | 29,032 | 3,786782609 | 8216,880939 | 1,331516743 | 9,013945968 |
| 4 | 44,236 | 5,769913043 | 16433,76188 | 1,75265701 | 9,707093149 |
| 6 | 56,545 | 7,375434783 | 24650,64282 | 1,998154854 | 10,11255826 |
| 8 | 67,932 | 8,860695652 | 32867,52376 | 2,181625278 | 10,40024033 |
| 10 | 77,69 | 10,13347826 | 41084,4047 | 2,315844622 | 10,62338388 |
| 12 | 86,5 | 11,2826087 | 49301,28563 | 2,423262487 | 10,80570544 |

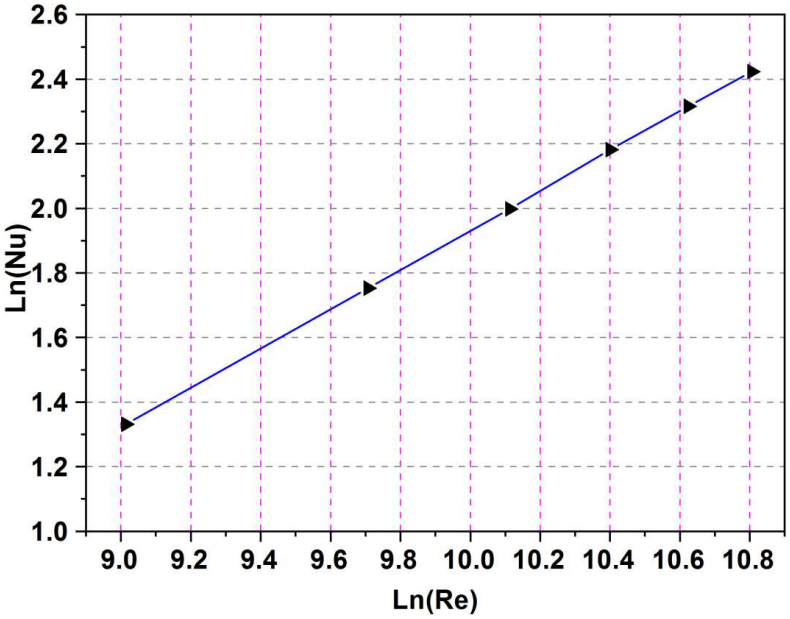


**Fig.8.** Theoretical relationship between *ln(Nu)* and *ln(Re).*

## 8. Conclusion

The new design heat flux sensor allows the in-time survey of various climatic factors such as;(wind, sun, rain, evaporation...), through the evolution of the global heat transfer coefficient and equivalent ambient temperature. The thermal sensor numerical simulation with air flow in a turbulent wind tunnel has shown the expected behaviour of the heat transfer coefficient h0 evolution.

We have studied numerically and theoretically a dynamic thermal flux sensor. According to this study, some conclusions can be given:

- The numerical simulation can be effectively used to simulate the thermal exchange in heat flux sensor, although numerical simulations were conducted in unstable turbulent flow status
- Our numerical simulation results show the heat transfer coefficient values 19% large than the ones obtained theoretically, and the heat transfer coefficient values 10% smaller than the ones obtained experimentally.

**References:**

[1] Van der Graff F, F. 1990, Heat flux sensors, in Ricol, T. and Scholz, J. (eds), Thermal Sensors 4, VCH, Weinheim, Germany-(1990) 297–322.

[2] Devisme J M, T Langlet, O Douzane, J M Roucoult, M Quéneudec, “Etude théorique et expérimental de fluxmètres à gradient transversal pour la thermique du bâtiment”, Int. J. Therm. Sci. 40 (2001)205-215

[3] Mityakov A V, S Z Sapozhnikov, V Y Mityakov, A ASnarskii, M I Zhenirovsky, J JPyrhonen, “Gradient heat flux sensors for high temperature environments”, Sens Actuators A, 176 (2012) 1-9

[4] Ewing J, A Gifford, D Hubble, P Vlachos, A Wicks, T E Diller, “A direct measurement thin film heat flux sensors array”, Meas. Sci. Technol, 21 (2010) 105201 (8pp)

[5] Mukherjee S K, M K Sinha, B Pathak, S k Rout, P K Barhai, A K Balamurugan, A K

Tyagi, F L Ng, “Invistigations on the structure, composition and performance of nanocrystalline thin film thermocouples deposited using anodic vacuum arc”, Thin silid films 518 (2010) 5839-5854

[6] therton J J A, M C Rosamond, S Johnstone, D A Zeze, ”Thermal characterisation of μL volume using a thin film thermocouple based sensor”, Sens Actuators A,166 (2011) 34-39

[7] Atherton J J, M C Rosamond, D A. Zeze, “A leaf-mounted thermal sensor for the measurement of water content”, Sensors and Actuators A 187 (2012) 67–72

[8] Mohammed H, H Salleh, M Z Yusoff, “Design and fabrication of coaxial surface junction thermocouples for transient heat transfer measurement”, Int. J. Heat Mass Transfer, 35 (2008) 853-859

[9] Mohammed H, H Salleh, M Z Yusoff, “The effect of scratch technique on the thermal-product value of temperature sensors”, Ahermophysics and Aeromechanics, 18 (2011) 51-64

[10] Serio B, H Gualous, J P Prenel, “A gold palladium thin film microsensor array for thermal imaging of laser beam waists”, Sensors and Actuators A, 84 (2000) 303-309

[11] Hamadi D, B Garnier, H Willaime, F Monti, H Peerhossaini, “A novel thin-film temperature and heat-flux microsensor for heat transfer measurements in microchannels”, Lab on a chip, 12 (2012) 652-658

[12] Hamadi D, H Ammar, B Garnier, M Brunet, H Willaime, F Monti, H Peerhossaini, “Nouvelle technique d’analyse des transferts de chaleur dans les microcanaux à l’aide de couches minces thermoresistives”, SFT 2010.

[13] He S, M mMench, S Tadigadapa, “Thin film temperature sensor for real time measurement of electrolyte temperature in a polymer electrolyte fuel cell”, Sens Actuators A, 125 (2006) 170-177

[14] Shannon M A, T M Leicht, P S Hrnjak, N R Miller, F A Khan, “Thin film resistances sensor for measuring liquid mass fraction in superheated refrigerant”, Sens Actuators A, 88 (2001) 164-177

[15] Kozlov A G, ”Analytical modeling of temperature distribution in resistive thin film thermal sensors”, Int. J. Therm. Sci, 45 (2006) 41-50

[16] Hamadi D, B Garnier, H Willaime, F Monti, H Peerhossaini, “A novel thin-film temperature and heat-flux microsensor for heat transfer measurements in microchannels”, Lab on a chip, 12 (2012) 652-658

[17] Pullins C A, T E Diller, “Adaptation of the in cavity calibration method for high temperature heat flux sensors”, Int. J. Heat Mass Transfer, 54 (2011) 3369-3380

[18] Pullins C A, T E Diller “In situ high temperature heat flux sensor calibration”, Int. J. Heat Mass Transfer, 53 (2010) 3429-3438

[19] Brunjail C., F Fragnaud F., “Capteur à impulsion pour la caractérisation des transferts thermiques entre une paroi et son environnement microclimatique en régime variable”, *Revue Phys. Appl.* 1982; 17:187-199

[20] Bertrand G, A. Ould El Moctara , B. Azeroua and A. Lahmarb.“New dynamic heat flux sensors to improve energy efficiency of buildings”*Polytech'Nantes.2014.*

[21] Nguyen N.T., “A novel thermal sensor concept for flow direction and flow velocity”, IEEE *Sensors Journal* 2005; 5:1224-1234

[22] Nguyen N.T., “A novel wind sensor concept based on thermal image measurement using a temperature sensor array”, *Sensors and Actuators A* 2004; 110:323-327

[23] Ruser H., Horn M., “Low cost weather sensor based on thermal impedance measurements”, *Instrumentation and Measurement Technology Conference*-IMTC May 1-3 Warsaw, Poland, 2007.
[24] Van der Graff, F. 1990, Heat flux sensors, in Ricol, T. and Scholz, J. (eds), Thermal Sensors 4, VCH,Weinheim, Germany-(1990) 297–322.
[25] Menter. F. R. 1993. "Zonal Two Equation k-ω Turbulence Models for Aerodynamic Flows", AIAA Paper 93-2906.
[26] Matyushenko, A.A. Garbaruk, A.V. Adjustment of the k-ω SST turbulence model for prediction of airfoil characteristics near stall. J.Phys. Conf.Ser. 2016, 769, 012082.
[27] Szpica D, GrzegorzMieczkowski, AndrzejBorawski, VitalisLeisis, SauliusDiliunas and TilmutePilkaite. The Computational Fluid Dynamics (CFD) Analysis of the Pressure Sensor Used in Pulse-Operated Low-Pressure Gas-Phase Solenoid Valve Measurements. Sensors (2021), 21, 8287.
[28] Calvet, P., LIOUSSE, F., Mesures locales de températures, pressions et vitesses au moyen de capteurs thermorésistants chauffés par impulsion. Revue Générale de Thermique n° 114 (juin 1971).